The Effect of the Rigidity of Perfluoropolyether Surfactant on Its Behavior at the Water/Supercritical Carbon Dioxide Interface

Lanyuan Lu and Max L. Berkowitz*

Department of Chemistry and NSF-STC-Environmentally Responsible Solvents and Processes, University of North Carolina at Chapel Hill, Chapel Hill, North Carolina 27599

Received: June 22, 2005; In Final Form: August 19, 2005

We performed a series of molecular dynamics simulations to study the PFPE (perfluoropolyether) and PE (polyether) surfactant monolayers at the water/supercritical carbon dioxide interface. Molecular differences between fluorocarbon surfactant PFPE and its hydrocarbon analogue PE were analyzed. We observed that values of intramolecular bonded interaction parameters which are related to chain rigidity determine the monolayer surface pressure. We show that "good" and "bad" properties of PFPE/PE surfactants are connected to conformational entropy. These results are consistent with our previous micellar simulations.

Introduction

Supercritical carbon dioxide ($scCO_2$) is a potentially excellent "green" solvent due to its nontoxicity, recyclability, and tuneability. Unfortunately, many solutes do not dissolve in $scCO_2$. To deal with this obstacle, one can create water in CO_2 (w/c) microemulsions to promote the solubility of solutes. Thus, a need exists in finding surfactant molecules that will facilitate creation of reverse micelles in pure $scCO_2$. Recently, substantial progress in this direction was accomplished through the use or design of a number of fluorinated or partially fluorinated surfactants.[1] In their turn, fluorinated surfactants are environmentally unfriendly and therefore cannot be utilized in high quantities. Nevertheless, we should study these surfactants to understand what makes them act as "good" surfactants in $scCO_2$ and design environmentally friendly "good" surfactants by imitating properties of fluorinated surfactants and their behavior in $scCO_2$.

The main issue related to special properties of fluorinated surfactants in $scCO_2$ is still not understood. Initially, the belief was that specific interactions between fluorinated tails of the surfactant molecules and CO_2 solvent were responsible for the "good" behavior of surfactants, but the ab initio calculations[2] and experiments[3] indicated that such specific interactions do not exist and that the strength of the tail solvent interactions was the same for hydrogenated and fluorinated surfactants. Recently, Stone et al.[4] proposed that the fractional free volume (FFV) available to CO_2 molecules in the tail region can serve as an index for the activity of the surfactant at the water/$scCO_2$ interface. According to Stone et al. the necessary condition for the surfactant to be able to create w/c microemulsion is to have a low FFV. Indeed, most of the examples discussed by Stone et al. demonstrate the usefulness of the FFV concept. Nevertheless, use of only FFV criteria for the determination of the ability to create microemulsions may be incomplete. For example, consider one of the popular fluorinated surfactants: perfluorinated polyether ammonium carboxylate surfactant (PFPE−$COO^-NH_4^+$, MW = 695.13). It has a relatively high FFV equal to 0.59, but it is a "good" surfactant, while a "bad" surfactant DiH8, which is a hydrogenated analogue of a fluorinated surfactant DiF8,[5] has a very similar FFV equal to 0.61.[4]

Micelles with PFPE and its hydrogenated analogue PE were the subject of previous simulations performed in our group.[6,7] In the first set of simulations[6] we preassembled the micelles and studied their properties. We observed that the presence of PFPE surfactant generated a nice reverse micelle in CO_2 with water molecules located in a water pool in the micellar interior. The direct contact between water and CO_2 in the reverse micelle was observed to be very small. In the simulations with the PE surfactants, a clustering of PE molecules was observed, and "patches" of a direct water/CO_2 contact appeared. In another set of simulations[7] the micelles were not preassembled, but were self-assembled, thus avoiding creation of artifacts due to the preassembly procedure. The results from our self-assembled and preassembled simulations were very similar and reached the same conclusion: "patches" of direct water/CO_2 contact on micellar surfaces created in the presence of PE surfactants raised the interface tension, which was responsible for the "bad" behavior of the PE surfactant.

It is hard to calculate and study the surface tension in micellar systems due to the presence of a pronounced interface curvature in these cases. Therefore we decided to learn about the relative properties of PFPE versus PE surfactants by performing monolayer simulations for which surface tension can be easily calculated. The results of this study are described below.

Simulation Details

We performed a number of molecular dynamics simulations to understand the difference between PFPE and PE surfactants. The simulations were done on systems containing surfactant monolayers at the $H_2O/scCO_2$ interface. As in our previous simulations, we used here the consistent valence force field (CVFF) parameters to describe the surfactant anions.[8] Accelrys's Material Studio software was used to calculate the point charges.[9] The OPLS set of intermolecular parameters was used to describe the NH_4^+ counterions[10] and a well-known SPC/E model was used to describe water molecules.[11] The parameters for the force field we used in our simulations to describe surfactant anions, counterions, and water can be found in Table 1 of ref 6. For computational economy a simple Lennard-Jones

* Address correspondence to this author. E-mail: maxb@unc.edu. Phone: 919-942-1161.

10.1021/jp053384u CCC: $30.25 © 2005 American Chemical Society
Published on Web 11/01/2005

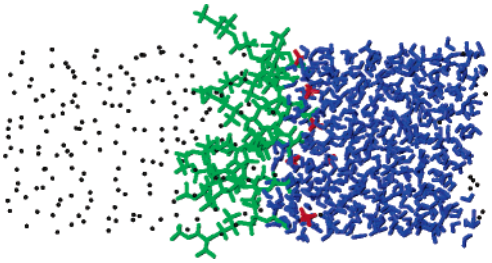

Figure 1. Snapshot of PFPE monolayer simulation at $t = 15$ ns. Blue particles are water molecules, green ones are surfactant molecules, red ones are NH_4^+ cations, and black ones are CO_2 molecules.

model was used to describe CO_2 molecules.[12] Gomes et al.[13] calculated the chemical potential of CO_2 in bulk fluorocarbons and hydrocarbons. They found that the partial charges on CO_2 described by the EPM2 model[14] played only a minor role in determining the value of the chemical potential. This fact somewhat justifies our usage of a single site uncharged sphere for CO_2 molecules in our simulations. More justification follows from the observation that in the previous simulations on reverse micelles containing either PE or PFPE surfactants performed in our group,[6, 7] the structural results were similar when the model for CO_2 was the three-site EPM2 model[6] and when it was a single-site Lennard-Jones sphere.[7]

In our simulations the systems contained 196 CO_2 molecules, 324 water molecules, and 9 surfactant molecules. The cubic simulation box contained water and CO_2 regions. Because of the periodic boundary conditions two interfaces were present in the system. One interface is between water and $scCO_2$, the second interface is also between water and $scCO_2$, only modified by the presence of nine surfactant molecules. A snapshot of a simulation with a PFPE monolayer is shown in Figure 1. All simulations were performed under constant normal pressure (NP_nAT ensemble was used and the normal pressure P_n along the z axis was equal to 20 MPa, the same pressure as in our micellar simulations[6]). The cross section A in the xy plane was chosen in such a way that the area per headgroup in monolayer simulations was the same as the one in the PFPE micelle simulation (69.5 Å^2). The initial configuration of the monolayers we simulated had nine carboxyl carbons of the surfactant headgroup initially distributed on a lattice in the xy plane of the interface and all surfactant molecules in trans conformations. Each simulation lasted 30 ns: 10 ns of these were spent on equilibration and 20 ns on data collection. We used the pressure difference formula[15] to calculate the surface tension of each surfactant-modified interface. Since there are two interfaces in each simulation box we subtracted the surface tension calculated for the CO_2/water interface from the total surface tension to get the surface tension of the monolayer.[16]

In all simulations the temperature was 298.15 K and the time step was 2 fs. The long-range forces were calculated by using the Particle-Mesh Ewald[17] with a cut off for the direct Coulomb interaction and van der Waals interaction having a value of 0.9 nm. The constant normal pressure was maintained by coupling to the Parrinello−Rahman barostat[20,21] and the constant temperature by coupling to the Nose−Hoover thermostat;[18,19] both coupling constants were 0.5 ps. All simulations were performed with the GROMACS MD package.[22]

Results and Discussions

Surface Tension Calculations. The ability of certain surfactants to decrease the surface tension of the interface can serve as an index of the efficiency of these surfactants. Usually the value of the surface tension reduction, $\gamma_0 - \gamma$ (γ is the surface tension in the presence of the surfactant molecules; γ_0 is the surface tension for the pure liquid/liquid interface) depends on a surfactant concentration. At a particular concentration, the large value for the surface tension reduction stands for high surfactant efficiency. Since PFPE is an efficient surfactant, we expect that the simulated system containing the PFPE modified $scCO_2$/water interface has a lower surface tension than the system containing the pure $scCO_2$/water interface. As we can see from Table 1, this is indeed the case for the surface tension of the PFPE modified interface. At the same time we observed that the surface tension of the PE modified interface was even higher than that of the $scCO_2$/water interface in our simulation. Here we notice that the values of the surface tension in our simulations are higher than the values from other simulations reported in the literature.[23,24] Comparison with the results from a simulation performed on a system containing pure $scCO_2$/H_2O interface, with CO_2 modeled by a three-site EPM2 model,[14] showed that the increase in the value of surface tension is due to the single-site CO_2 model that we used. Note that our simulation is performed at a slightly lower temperature compared to the one in the simulation of da Rocha et al.,[23] which may also be the reason for the higher value of our surface tension. Although it is nice to obtain in simulations the values for the surface tension that are close to the experimental one, our main interest in this work is to observe the trends in the change of these values as we add different surfactants to the $scCO_2$/H_2O interface. Since in our simulations the PFPE modified interface has a lower surface tension compared to the $scCO_2$/water interface, we therefore conclude that our model of PFPE is a model of a "good" surfactant. As we can also see from Table 1, the presence of PE surfactant produces a slight increase in the surface tension of the interface with the surfactant compared to the surface tension of the pure interface. This means that in our system containing the PE monolayer, the surface pressure of the monolayer is negative and the monolayer will shrink, if the external pressure is not applied. Such shrinkage of the monolayer is consistent with the creation of a "patch" we observed previously in our micelle simulations.[6,7] Both the negative surface pressure and the "patch" in the micelle will not be observed in experiments where the surfactant concentration and the size of the system are very different. The slight increase (or at least no reduction) in the surface tension of the interface we observe in the presence of the PE surfactant is the signature of a "bad" surfactant.

TABLE 1: Results for the Surface Tension Calculations[a]

surfactant on interface	surface tension (mN/m)
no surfactant	47.6 ± 1.4
PFPE	33.6 ± 2.2
PE	52.2 ± 2.2
A1	38.7 ± 1.4
A2	52.6 ± 0.6
PFPE with no partial charge on tail	29.8 ± 1.5
PE with no partial charge on tail	50.6 ± 2.2
PFPE with hydrogenated head[b]	40.1 ± 0.9
PFPE with no partial charge on first two F atoms	40.9 ± 0.6

[a] The standard deviation is obtained by using a block average method with 4 blocks for each simulation. Here the definition of "head" includes the first $-CF_2/-CH_2$ group. [b] The first two F atoms LJ parameters and partial charges were changed to those of H atoms on PE.

What is the reason that PFPE is a "good" surfactant and PE is a "bad" surfactant? To answer this question, first notice that the surface pressure and the free energy of the system containing a monolayer at the liquid water/liquid CO_2 interface can be

written as:[25]

$$\pi = \left(\frac{\partial F_m}{\partial a}\right)_{T,n_m} \quad (1)$$

$$F_m = n_m\phi_m(a) = n[\phi_{\text{hyd}}(a) + \phi_{\text{int}}(a) + \phi_{m-u}(a)] \quad (2)$$

where a is the area per surfactant molecule. The three terms in (2) are contributions from the headgroup hydration, surfactant interaction (including intramolecular interaction), and surfactant tail-upper phase (CO_2) interaction, respectively. Since the division of the surfactant molecule into the headgroup and tail regions cannot be done uniquely, the relative contribution of the three terms depends on the convention used for the definition of the regions.

To understand the difference between PFPE and PE surfactants and the relative contributions of different terms in eq 2, we performed several computational experiments. In these experiments we changed various parameters in the surfactant force field to observe the influence due to the changes in electrostatic interaction, Lennard-Jones interaction, and the molecular geometry.We performed a number of simulations where we varied the parameters in the force field from the ones describing PFPE to the parameters describing PE or vice versa. After we performed our test runs we found that by changing the PE's bonded parameters to those of PFPE's we can produce a "good" surfactant. Here the bonded parameters in the force field refer to the parameters such as bond length, bond angle, etc. The expression for the bonded energy containing bonded parameters is:

$$U_{\text{bond}} = \sum_i k_{b,i}(r_i - r_0)^2 + \sum_i k_{\theta,i}(\theta_i - \theta_0)^2 + \sum_i A_i[1 + \cos(m\phi_i - \phi_0)] + \sum_i B_i[1 + \cos(n\chi_i - \chi_0)] \quad (3)$$

The CVFF that we use to describe surfactant anions is constructed in such a way that the difference in the bonding parameters describing PFPE and PE is in the values of the bond stretching parameters $k_{b,i}$ and angle distortion parameters $k_{\theta,i}$, and also in the values of the equilibrium bond lengths and angles, while the torsion A_i and the out-of-plane B_i parameters remain the same. The nonbonded term in the energy contains contributions from the Coulomb interaction energy of partial charges and Lennard-Jones interaction energy. The nonbonded parameters for PFPE are different from the ones for PE. We observed that the data looked especially clear when we considered simulations with only two "artificial" surfactants. The first artificial surfactant had the same bonded parameters as PFPE and the same nonbonded parameters as PE. We called this surfactant molecule A1 in the paper. The second artificial molecule, A2, had the same bonded parameters as PE and the same nonbonded parameters as PFPE. As we can see from Table 1, the interface with A1 has a surface tension that is lower than the tension for the pure CO_2/water interface, and the value of the surface tension is close to that of PFPE. This indicates that A1 is a "good" surfactant. On the contrary, the interface with A2 has a high surface tension, similar to the one with PE. Since the surfactants with the same vdW and partial charge parameters can have very different surfactant performance, we conclude that these parameters are not the only parameters that determine the surfactant performance. As we can see the bonded parameters play a very important role.

The conformational distribution of the surfactants also plays an important role. In Table 2 we calculated the average tail−tail intermolecular energy (Coulomb plus LJ) using the system trajectories. Here the definition of "tail" incorporates the surfactant molecule without the $-CO_2^-$ group. We can observe from the data that all the energy values are negative indicating that the cohesive energy term plays the dominant role. We observe that "good" surfactants (PFPE and A1) display a less negative interaction energy compared to "bad" surfactants (PE and A2). This indicates that the conformational distribution of the tails in "good" surfactants is different from that of the "bad" surfactants and that it is possible that tails in "bad" surfactants are in a more condensed state.

TABLE 2: The Average Tail−Tail Interaction Energy for Monolayer Systems (kJ/mol)

PFPE	PE	A1	A2
−435.03	−555.50	−334.03	−480.24

To understand the influence of electrostatic tail−tail interactions we also performed simulations with charges on tails removed. Here we used the same definition of "tail" and "head" as in our group's previous paper[6] (e.g. for the PFPE anion the "head" contained the CO_2^- group, the first CF_2 group, and the first ether oxygen). The partial charges on headgroup ether O atoms were modified to keep the whole system at zero net charge. We observed that the big difference between surface tension in systems with PFPE and PE still remained. This fact suggests that our group's previous conclusion[6] about a strong electrostatic attraction between PE tails may be incorrect. The influence from the tail dipole is very small compared to that of other factors. The influence of the partial charges on the first two PFPE fluorine atoms which can be considered to be part of the headgroup can be seen from the last two rows in Table 1. As we can see from this table, the main change in the surface tension is due to the removal of the partial charge on fluorine. The important role of this partial charge is not difficult to understand since the headgroup partial charge can change both the headgroup Coulomb repulsion term and the headgroup hydration term in the free energy expression. We want to emphasize that all our discussions about the role of partial charges are focused on the surfactant−surfactant interactions. The surfactant−CO_2 electrostatic interaction is expected to be unimportant for the total free energy as was reported in the literature.[13]

Our computational experiments on artificial surfactants indicate the importance of the chain conformations for the effectiveness of the surfactant. Changes in conformations may be accomplished by variation of the Lennard-Jones size parameter, charges, and changes in bonding parameters. We observed that size parameters and partial charges are not the only important parameters that describe the tail−tail intermolecular interactions as one may naively assume and that changes in bonding parameters play a major role in determining the effectiveness of the surfactant. The values of partial charges on the tail atoms do not have a big influence on the surface tension. Partial charges on the first $-CH_2$ or $-CF_2$ groups do have a certain influence.

2D Distribution of Surfactant Headgroups. In our previous simulation of the micellar systems[6,7] we found that PFPE surfactants uniformly distribute themselves on the approximately spherical $scCO_2$/water interface in a typical micellar configuration. PE surfactants, on the contrary, tend to cluster together, therefore leaving "patches" where a direct $scCO_2$/water contact on the spherical interface occurs. The results from our monolayer simulations can be linked to these observations, meaning that an effective repulsion exists between PFPE molecules, while

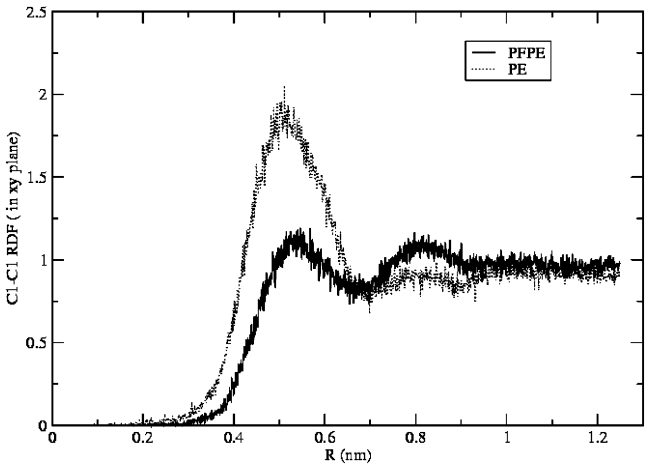

Figure 2. Two-dimensional (in *xy*-plane) radial distribution functions for C_1-C_1 atoms.

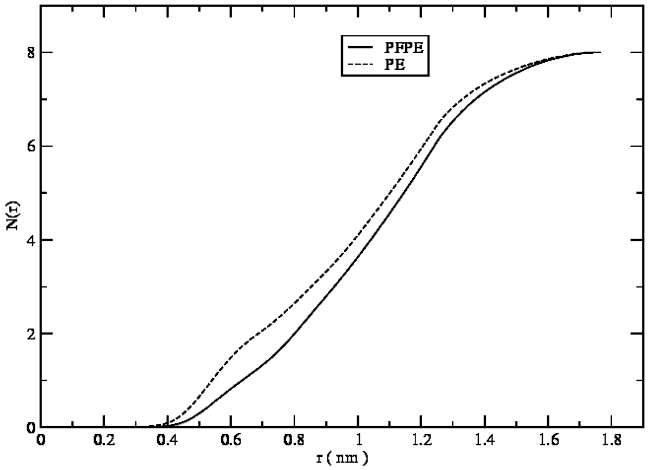

Figure 3. Average number of other C_1 atoms $N(r)$ within a distance r from a central C_1 atom.

an effective attraction should exist between PE molecules. Indeed, we observed a positive surface pressure for the PPFE monolayer, which indicates effective repulsion between molecules and keeps the surfactant distribution uniform. The surface pressure is negative for the PE monolayer, which produces an effective attraction between surfactants and their cluster distribution.

Since we used the same conditions for the micellar and monolayer simulations, we anticipated to see a difference in the distributions of PE versus PFPE surfactants in our monolayer simulations as well. Although we were not able to observe a patch of direct $scCO_2$/water contact in monolayer simulations, due to a rather small number of surfactant molecules in our simulation box, the analysis showed that the distribution of fluorinated and hydrogenated surfactant in monolayers is different indeed. To understand this difference, we first studied the distribution of the surfactant headgroups. The 2-dimensional radial distribution function (rdf) of the surfactant headgroups is shown in Figure 2. The index that denotes the carbon atom in this work is the same as that in our group's previous work.[6] C_1 to C_9 are backbone carbon atoms starting from carboxyl carbon C_1. C_{10} to C_{12} are side chain carbons. As we can see from this figure the amplitude of the first peak for the PE surfactant is larger than the corresponding amplitude for the PFPE surfactant, which means that the probability of finding the PE molecules in close contact is higher if compared to the probability for the PFPE molecules. Also, in the PFPE case the amplitude of the first peak is similar to the amplitude of the second peak and both of them are close to unity. This means that the distribution of the PFPE surfactants is more uniform. We also calculated the number of nearest neighbors around the surfactant headgroups. This information is displayed in Figure 3. As we can see from this figure, there are more PE headgroup neighbors within a short distance from a central headgroup. This is consistent with a cluster distribution of the PE surfactants.

Because the distribution of the PFPE molecules is uniform, there is, on average, more empty space available between the tails of these molecules. As a result the CO_2 solvent molecules can penetrate more efficiently into this space. Therefore we expect that more CO_2 molecules can be found in the PFPE's tail region, meaning better solubility of PFPE in CO_2. To check this expectancy we counted the total number of CO_2 molecules in any surfactant's first solvation shell, as we did in our previous work.[6] As we can see from Table 3 there are indeed more CO_2 molecules in the first solvation shell of the PFPE surfactant.

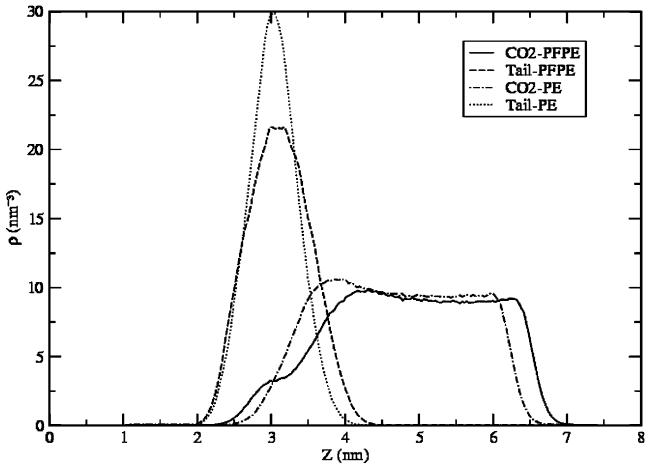

Figure 4. Number density for the surfactant tails and CO_2. Each CF_n/CH_n and O was counted as a group.

TABLE 3: Number of CO_2 Molecules in the First Solvation Shell of Surfactant Tails in Monolayer Simulations

	PFPE	PE	PE (headgroup fixed)
no. of CO_2	62 ± 6	50 ± 6	62 ± 5

This suggests a larger CO_2 penetration into the tail region. We can also observe this penetration from the density profile (Figure 4). This figure shows that the density curve for CO_2 drops significantly after entering the tail region for both PFPE and PE cases. Nevertheless, some substantial differences can be seen from the figure; there is a stable region in the PFPE case with a plateau region indicating the CO_2 penetration. On the basis of the numbers from Table 3 and the values of the tail/CO_2 interaction energy, we observe that the conclusion reached previously in the literature that there is no special affinity between fluorocarbon and CO_2[13] is also applicable in our case. The average tail/CO_2 interaction energies in our monolayer simulations are -514.57 and -430.17 kJ/mol for PFPE and PE cases, respectively. If we assume that the interaction is mainly due to CO_2 molecules located in the first solvation shell, we can calculate the interaction energy per each CO_2 molecule in the first solvation shell. The results are -8.30 and -8.60 kJ/mol for PFPE and PE, respectively, meaning that in our simulations the interaction between PE and single CO_2 is approximately the same as the interaction between PFPE and

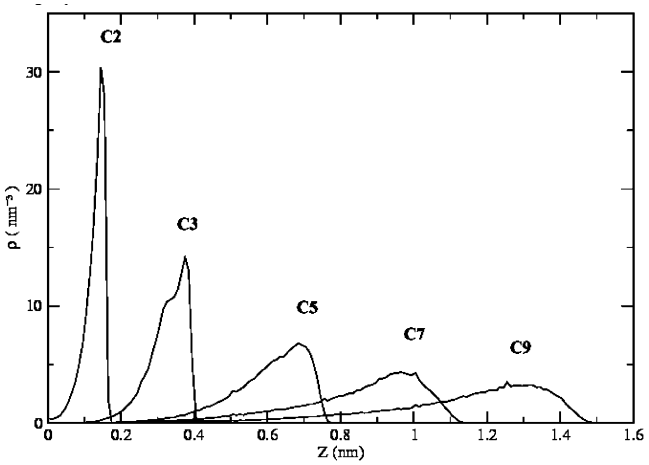

Figure 5. Number density for the PFPE backbone carbon atoms as a function of distance to the headgroup.

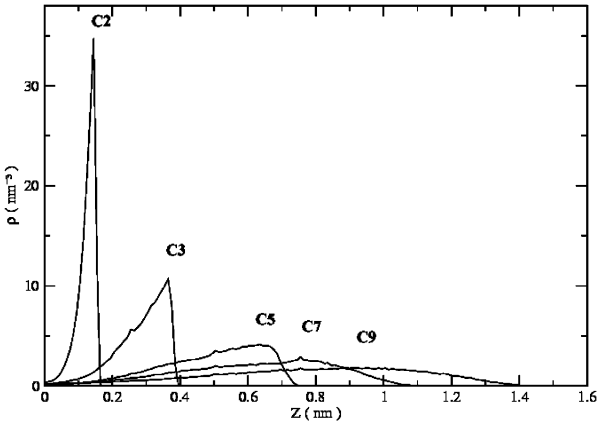

Figure 6. Number density for the PE backbone carbon atoms as a function of distance to the headgroup.

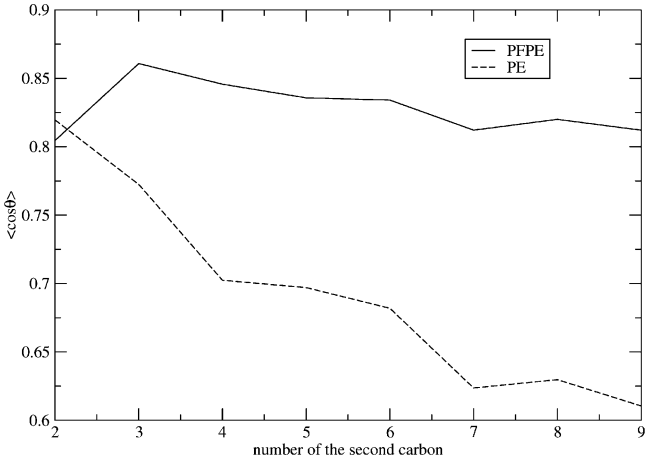

Figure 7. The average cosine of the angle formed between the vector normal to the interface and the vector connecting C_1-C_i.

single CO_2. The larger total negative tail/CO_2 interaction energy in the PFPE case is due to a larger number of CO_2 molecules in the solvation shell of the surfactant molecule.

Tail Conformations and Chain Rigidity. As our previous discussion showed, the intermolecular interactions are not the crucial ones that can explain the surface activity of PFPE or PE surfactants. Indeed, as we saw previously, the A1 molecules that have the same intramolecular force field parameters as PFPE and the same intermolecular force field parameters as PE display high surface activity and are "good" surfactants, while A2 molecules that have the same intermolecular parameters as PFPE and the same intramolecular parameters as PE are "bad" surfactants. Intramolecular force field parameters determine the flexibility of the molecules, and consequently, the conformations of the surfactant tails. The strong dependence of the results on the choice of the intramolecular parameters shows that in the case of PFPE/PE surfactants flexibility plays a very important role in the monolayer behavior and its surface activity. Compared to PE molecules, the PFPE molecules are more rigid and they pack and distribute themselves so as to leave more space between tails. The CO_2 molecules can enter this space due to the tail/CO_2 interaction. In their turn the CO_2 molecules push the surfactant molecules away from each other. Thus, we observe that the PFPE surfactants have a uniform 2-dimensional distribution of the headgroups and the system displays a positive surface pressure. The tails of the PE molecules are not so rigid and as a result their conformations are more disordered. The more disordered tails do not leave enough room for the CO_2 molecules to enter. Due to the attraction of the PE tails the surfactants undergo cluster formation. In addition, the CO_2 molecules outside the clusters (in the "patch" region) can also push the surfactants toward each other. As a result, we observe that the PE surfactants display an effective attraction, and a system has a negative lateral pressure in this case.

To check the difference in the conformations of PFPE and PE tails, we performed a conformational analysis of our monolayer simulation trajectories. In Figures 5 and 6 we plotted the number density profiles of backbone atoms with their distances calculated relative to the position of the headgroups C_1. Compared to the profile for the PFPE, there are more overlaps seen in the profile of the PE. We also observe broader density distributions in the PE profile, indicating that more disorder is present in the PE monolayer compared with that observed in the PFPE monolayer. The same conclusion on disorder can be obtained from observing the tail density profiles in Figure 4. We also plotted the cosine of the angle between the vector connecting C_1-C_i and the vector normal in order to study the orientation of each segment in the tail. From Figure 7 we observe that the orientation of the PFPE tail is basically perpendicular to the interface, although a small tilt angle is present in this case. In the PE case there is an obvious tilt angle for the whole tail. To check the order of each segment, the order parameter

$$S_{CF} = \frac{3}{2}\langle \cos^2\theta \rangle - \frac{1}{2} \tag{4}$$

(θ is the angle between the CF(CH) bond and the normal to the interface) for each carbon along the chain was plotted in Figure 8. As we can see, as the carbon number increases, both PPFE and PE chain segments become more disordered, although the order parameters for the carbons in the PE chains are closer to zero, especially for the last several carbon atoms in the surfactant tails. This confirms the fact that PE tails have a more disordered configuration than PFPE tails. The backbone dihedral trans/gauche ratio can also serve as an important index for the degree of disorder of the surfactant tails. We show in Table 4 that the PE tails have a higher percentage of gauche defects which is consistent with our previous discussion. To support our qualitative discussion with a quantitative argument we performed an additional simulation on a PE surfactant monolayer with the headgroup carbon atoms C_1 uniformly distributed on a lattice and fixed during the simulation. The results of this simulation were analyzed and compared with the results of the simulation on the PE monolayer. We calculated the energy and

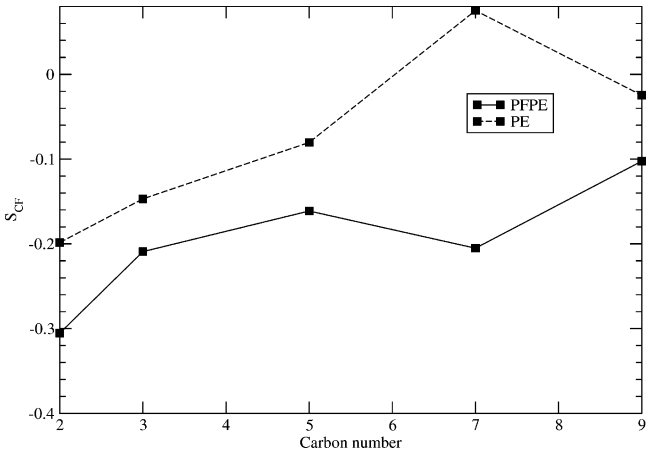

Figure 8. The order parameter for the CF(CH) bond.

TABLE 4: The Gauche/Trans Ratio for the Surfactant Backbone Dihedrals in Monolayer Simulations

	PFPE	PE	PE with fixed headgroups
g/t ratio	0.296	0.373	0.308

TABLE 5: Energy and Entropy Change for Monolayers When Transforming from a State with the PE Headgroups Fixed to a Normal Unconstrained Monolayer (in kJ/mol)

ΔE_{t-t}(tail/tail)	−78.28
ΔE_{t-w}(tail/{water + cation})	−1.03
ΔE_{t-c}(tail/CO_2)	68.4
$-T\Delta S_{tail}$	−441.32

entropy changes for the monolayer tails when going from a system containing the PE monolayer with fixed headgroup atoms to a system with unrestricted distribution of the headgroup carbon atoms. The results are listed in Table 5. The entropy change was calculated based on the method of Schlitter.[26] As we can see from the data in Table 5, there is a negative energy change for the tail/tail interaction when going from a uniform distribution to a cluster distribution, which is caused by the mutual tail approach. Since due to this motion the space between tails is reduced in cluster configuration and the number of CO_2 molecules is pushed out from this space, the number of CO_2 molecules solvating the tail is also reduced, which causes a positive energy change in tail−CO_2 interaction. Basically, the two changes cancel each other. The change in tail/aqueous solvent interaction energy is very small and contributes very little to the energy balance. Table 5 shows that compared to the energy change, the entropy change is dominant. Thus, the entropic contribution to the free energy change should be considered to be the main driving force for the formation of the cluster configuration.

We also calculated a trans/gauche ratio for surfactants with fixed PE. The result (see Table 4) shows that PE monolayer tails are more ordered when monolayer headgroups are fixed in a uniform configuration. These trans/gauche data are consistent with the entropy change. Although this result may seem to be somewhat unusual (surfactant tails usually become more disordered with an increase in the area per surfactant[27]), it can be easily explained. As Table 3 shows, the number of CO_2 molecules in the solvation shell of the fixed PE monolayer is larger than that in the unrestricted monolayer. A larger number of CO_2 molecules around the surfactant enforces the surfactant to adopt a more ordered conformation.

Conclusions

We performed MD simulations on systems containing monolayers of perfluorinated polyether ammonium carboxylate surfactant (PFPE−$COO^-NH_4^+$, MW = 695.13) and its hydrogenated analogue PE−$COO^-NH_4^+$ situated at the water/scCO_2 interface to study the difference between the fluorinated and hydrogenated surfactants in order to explain their different surface activity. By changing the force field parameters that are responsible for the relative strength of intra- and intermolecular interactions, we studied the influence of these interactions on the value of the surface tension. We found that intramolecular interactions and molecular geometry play an important role in the surface activity of a "good" surfactant. Our simulation results are consistent with the results from the previous simulations on the reverse micellar systems performed in our group. We observed that the difference in the values of the surface tension for the fluorinated and hydrogenated surfactants corresponds to different 2-dimensional headgroup distributions for the PFPE and PE surfactants. These different distributions are seen in both micellar and monolayer simulations. While in the PFPE case the simulations show that surfactants are distributed uniformly, the PE surfactants are clustering. Various types of analyses were performed in order to reveal the difference in tail conformations of PFPE and PE molecules. We found that the more rigid PFPE tails can provide more space between the surfactant tails for CO_2 molecules to occupy this space. Thus the PFPE tails can be well solvated in CO_2 solvent and as a consequence we observed uniformly distributed PFPE surfactants and the interface had a low surface tension. The more flexible PE tails are more disordered; this leaves less space for the CO_2 molecules to penetrate between the surfactant tails, thus explaining the low solubility of these surfactants in CO_2. We also performed energy and entropy calculations for the PE molecules when their headgroups were restricted to a lattice configuration on the interface plane. The positive change in the tail conformational entropy for these molecules when going from a restricted to an unrestricted state of motion in the plane of the interface is, in our opinion, the driving force for the formation of cluster configuration in the PE system. This driving force is not available in the case of PFPE because these surfactants have a rigid tail. How important is this entropic effect for the other surfactant molecules should be a subject of future studies. We feel that the described effect should be considered together with other effects, such as surfactant excluded volume and cohesive energy when designing effective surfactants for scCO_2.

Acknowledgment. This work was supported by the Kenan Center for the Utilization of Carbon Dioxide in Manufacturing and the STC Program of the National Science Foundation under Agreement CHE-9876674.

References and Notes

(1) Eastoe, J.; Dupont, A.; Steytler, D. C. *Curr. Opin. Colloid Interface Sci.* **2003**, *8* (3), 267−273.

(2) Diep, P.; Jordan, K. D.; Johnson, J. K.; Beekman, E. J. *J. Phys. Chem. A* **1998**, *102* (12), 2231−2236.

(3) Yonker, C. R.; Palmer, B. J. *J. Phys. Chem. A* **2001**, *105* (2), 308−314.

(4) Stone, M. T.; Smith, P. G.; da Rocha, S. R. P.; Rossky, P. J.; Johnston, K. P. *J. Phys. Chem. B* **2004**, *108* (6), 1962−1966.

(5) Stone, M. T.; da Rocha, S. R. P.; Rossky, P. J.; Johnston, K. P. *J. Phys. Chem. B* **2003**, *107* (37), 10185−10192.

(6) Senapati, S.; Berkowitz, M. L. *J. Phys. Chem. B* **2003**, *107* (47), 12906−12916.

(7) Lu, L.; Berkowitz, M. L. *J. Am. Chem. Soc.* **2004**, *126* (33), 10254−10255.

(8) Dauber-Osguthorpe, P.; Roberts, V. A.; Osguthorpe, D. J.; Wolff, J.; Genest, M.; Hagler, A. T. *Proteins* **1988**, *4* (1), 31−47.

(9) *Discover User Guide Part I*; Biosym Technologies, San Jose, CA, 1993.

(10) Jorgensen, W. L.; Gao, J. *J. Phys. Chem.* **1986**, *90* (10), 2174−2182.

(11) Berendsen, H. J. C.; Grigera, J. R.; Straatsma, T. P. *J. Phys. Chem.* **1987**, *91* (24), 6269−6271.

(12) Higashi, H.; Iwai, Y.; Uchida, H.; Arai, Y. *J. Supercrit. Fluids* **1998**, *13* (1−3), 93−97.

(13) Gomes, M. F. C.; Padua, A. A. H. *J. Phys. Chem. B* **2003**, *107* (50), 14020−14024.

(14) Harris, J. G.; Yung, K. H. *J. Phys. Chem.* **1995**, *99* (31), 12021−12024.

(15) Rowlinson, J. S.; Widom, B. *Molecular Theory of Capillarity*; Clarendon Press: Oxford, UK, 1982.

(16) Dominguez, H.; Berkowitz, M. L. *J. Phys. Chem. B* **2000**, *104* (22), 5302−5308.

(17) Essmann, U.; Perera, L.; Berkowitz, M. L.; Darden, T.; Lee, H.; Pedersen, L. G. *J. Chem. Phys.* **1995**, *103* (19), 8577−8593.

(18) Nose, S. *J. Chem. Phys.* **1984**, *81* (1), 511−519.

(19) Hoover, W. G. *Phys. Rev. A* **1985**, *31* (3), 1695−1697.

(20) Parrinello, M.; Rahman, A. *J. Appl. Phys.* **1981**, *52* (12), 7182−7190.

(21) Nose, S.; Klein, M. L. *Mol. Phys.* **1983**, *50* (5), 1055−1076.

(22) van der Spoel, D.; Lindahl, E.; Hess, B.; van Buuren, A. R.; Apol, E.; Meulenhoff, P. J.; Tieleman, D. P.; Sijbers, A. L. T. M.; Feenstra, K. A.; van Drunen, R.; Berendsen, H. J. C. *Gromacs User Manual*, version 3.2, 2004; www.gromacs.org.

(23) da Rocha, S. R. P.; Johnston, K. P.; Rossky, P. J. *J. Phys. Chem. B* **2002**, *106* (51), 13250−13261.

(24) da Rocha, S. R. P.; Johnston, K. P.; Westacott, R. E.; Rossky, P. J. *J. Phys. Chem. B* **2001**, *105* (48), 12092−12104.

(25) Marsh, D. *Biochim. Biophys. Acta−Rev. Biomembr.* **1996**, *1286* (3), 183−223.

(26) Schlitter, J. *Chem. Phys. Lett.* **1993**, *215* (6), 617−621.

(27) Szleifer, I.; Ben-Shaul, A.; Gelbart, W. M. *J. Phys. Chem.* **1990**, *94* (12), 5081−5089.